

1 **High pathogenicity avian influenza A (H5N1) clade 2.3.4.4b virus infection in a captive Tibetan black**  
2 **bear (*Ursus thibetanus*): investigations based on paraffin-embedded tissues, France, 2022**

3  
4 Pierre Bessière<sup>1\*</sup>, Nicolas Gaide<sup>1</sup>, Guillaume Croville<sup>1</sup>, Manuela Crispo<sup>1</sup>, Maxime Fusade-Boyer<sup>1</sup>, Yanad  
5 Abou Monsef<sup>1</sup>, Malorie Dirat<sup>1</sup>, Marielle Beltrame<sup>2</sup>, Philippine Dendauw<sup>2</sup>, Karin Lemberger<sup>3</sup>, Jean-Luc  
6 Guérin<sup>1</sup> and Guillaume Le Loc'h<sup>1</sup>

7  
8 <sup>1</sup> IHAP, Université de Toulouse, INRAE, ENVT, Toulouse, France.

9 <sup>2</sup>Réserve Africaine de Sigean, Sigean, France.

10 <sup>3</sup>Vet Diagnostics, Charbonnières-les-Bains, France

11 \*Corresponding author: [pierre.bessiere@envt.fr](mailto:pierre.bessiere@envt.fr)

12  
13 **Abstract**

14 High pathogenicity avian influenza viruses H5Nx (HPAIVs) of clade 2.3.4.4b have been circulating  
15 increasingly in both wild and domestic birds in recent years. In turn, this has led to an increase in the  
16 number of spillovers events affecting mammals. In November 2022, a HPAIV H5N1 caused an outbreak  
17 in a zoological park in the south of France, resulting in the death of a Tibetan black bear (*Ursus*  
18 *thibetanus*) and several captive and wild bird species. We detected the virus in various tissues of the  
19 bear and a wild black-headed gull found dead in its enclosure using histopathology, two different *in-*  
20 *situ* detection techniques and next generation sequencing, all performed on formalin fixed paraffin  
21 embedded tissues. Phylogenetic analysis performed on HA gene segment showed that bear and gull  
22 strains shared 99.998% genetic identity, making the bird strain the closest related one. We detected  
23 the PB2 E627K mutation in minute quantities in the gull, whereas it predominated in the bear, which  
24 suggests that this mammalian adaptation marker was selected during the bear infection. Our results  
25 provide the first molecular and histopathological characterization of an H5N1 virus infection in this  
26 bear species.

27  
28  
29  
30  
31  
32

## 33 Introduction

34 The genetic and antigenic diversity of influenza viruses is considerable: 16 and 9 hemagglutinin and  
35 neuraminidase subtypes respectively circulate in wild waterfowl, considered the reservoir of influenza  
36 viruses [1]. Following the acquisition of a mutation in the sequence encoding the hemagglutinin  
37 cleavage site, viruses belonging to the H5Nx and H7Nx subtypes are capable of acquiring a high  
38 pathogenicity phenotype. While the tropism of low pathogenicity avian influenza viruses (LPAIVs) is  
39 mainly restricted to the digestive and respiratory tracts, high pathogenicity avian influenza viruses  
40 (HPAIVs) can replicate systemically [2].

41  
42 For a long time, HPAIVs circulating in domestic birds were considered unlikely to return to the wild  
43 compartment: viruses adapt to the species they infect, and many viruses adapted to Gallinaceae are  
44 poorly adapted to wild waterfowl [3]. However, in recent years, this dogma has been shaken: HPAI  
45 H5Nx viruses, which initially appeared in the domestic compartment, have succeeded in becoming  
46 endemic in wild birds [4]. More importantly, while the species barrier between mammals and birds is  
47 considerable, these viruses have managed to cross it on several occasions.

48  
49 H5Nx HPAIVs' circulation, particularly those of clade 2.3.4.4b, has significantly increased in recent  
50 years: viruses of this clade are spreading in wild bird populations more rapidly than ever since their  
51 emergence in 1996 [5]. Thus, the occasions on which mammals have been exposed to the virus have  
52 become more frequent in turn. Infection generally occurs following exposure to contaminated feces  
53 or water, or animal carcasses [6]. Sporadic infections of wild mammals have been described in the past,  
54 but have never been as frequent as in recent years. Numerous domestic and wild animals have been  
55 contaminated, including various species of seals, sea lions, foxes, cats, raccoons, skunks and bears [7–  
56 12].

57  
58 These sporadic infections are not always dead ends [13], and every time an avian influenza virus  
59 manages to infect a mammal, there is a risk that adaptive mutations will appear [1]. When enough  
60 genetic changes accumulate, the result can be the emergence of a virus more efficiently transmitted  
61 between mammals. Ultimately, a novel influenza virus able to sustain transmission between humans  
62 could cause a pandemic [14].

63  
64 In November 2022, a Tibetan black bear (*Ursus thibetanus*) from the Sigean zoo in France was reported  
65 dead. Although infection with an avian influenza virus was not initially suspected, post-mortem  
66 analyses revealed the presence of clade 2.3.4.4b HPAIV H5N1 in various organs and blood. Over the  
67 following fortnight, several influenza-positive birds were also found dead nearby the bear enclosure,

68 suggesting a bird-to-bear transmission. Using formalin fixed paraffin embedded tissue, we conducted  
69 molecular and histopathological investigation to characterize this outbreak.

70

## 71 **Results**

### 72 *Outbreak detection*

73 In early November 2022, a 12-year-old male Tibetan black bear (*Ursus thibetanus*) was found dead in  
74 its enclosure at the Sigean zoo, France. A few days before, zookeepers had noticed a slight decline in  
75 general condition, while the day prior to its death, the bear presented marked dyspnea, hyperthermia,  
76 lateral decubitus and diarrhea. Analyses carried out by the zoo's veterinarians showed severe  
77 leukopenia and hypercreatininemia, consistent with acute renal failure (**Supplementary File 1**). A  
78 necropsy was carried out, revealing hemorrhagic lesions (petechiae and suffusion) on the epicardium  
79 and liver, severe congestion of lungs, kidneys and intestines, and finally, a necrotic tracheal mucosa.  
80 Over the following days, several zoo and wild birds (pelicans, jackdaws and gulls) died and tested  
81 positive by RT-qPCR for clade 2.3.4.4b HPAIV H5N1, one of the carcasses being found in the bear's  
82 enclosure: a black-headed gull (*Chroicocephalus ridibundus*), which the zoo veterinarians also  
83 necropsied (marked pulmonary and splenic congestion were the most remarkable findings identified  
84 at necropsy). In the days following the bear's death, other bears of the same species displayed mild to  
85 moderate clinical respiratory signs, but could not be sampled to be analyzed as part of this study.

86 The possibility that the bear might have been infected by an H5N1 virus of clade 2.3.4.4.b was  
87 subsequently suspected, and confirmed by molecular analysis of biological samples sent to the French  
88 reference laboratory for high pathogenicity avian influenza, which deposited the viral genome  
89 sequence on GISAID (isolate ID EPI\_ISL\_17233426). After initial routine screening at a diagnostic  
90 histopathology laboratory (Vet Diagnostics, France), formalin fixed paraffin-embedded (FFPE) tissues  
91 from the bear and gull were then sent to the ENVT laboratory for further investigation.

### 92 *Pathological examination of the infected bear and black-headed gull*

93 Histopathological examination of the bear revealed acute, marked multifocal to coalescing fibrino-  
94 necrotizing lymphadenitis and splenitis, associated with vasculitis and hemorrhages (**Figure 1**); marked  
95 pulmonary edema and congestion; moderate suppurative tracheitis with concurrent submucosal  
96 vascular thrombosis; severe, multifocal necro-suppurative hepatitis. Marked acute hemorrhages,  
97 involving the subepicardium and renal interstitium, were also present, while the gastro-intestinal tract  
98 appeared unremarkable (**Supplementary Figure 1**). Viral antigen and RNA were frequently detected in  
99 a visceral lymph node, multifocally, within areas of necrotizing vasculitis (**Figure 1**). In the lung, viral  
100 antigen was sparsely detected within bronchoalveolar luminal debris, lobular and interlobular  
101 interstitium admixed with non-specific background. Viral RNA was similarly detected in terms of

102 distribution, although the signal appeared more widespread within the pulmonary parenchyma (**Figure**  
103 **1**). In the kidney, viral antigen was rarely observed within a few glomerular tufts, while viral RNA  
104 detection was negative (**Supplementary Figure 1**). Additionally, RNAscope *in situ* hybridization  
105 revealed sparse viral RNA within interstitium of myocardium, gastro-intestinal and tracheal mucosa  
106 and submucosa and splenic red pulp. Other findings included myocardial atherosclerosis and  
107 mineralization.

108

109 Histopathological assessment of the gull showed acute necrotic-inflammatory changes in the majority  
110 of the organs examined. Mild to marked encephalitis, pancreatitis, splenitis, hepatitis, nephritis and  
111 thyroiditis lesions exhibited variable amounts of viral antigen and RNA highlighted by IHC and  
112 RNAscope ISH, respectively (**Supplementary Figures 2 and 3**).

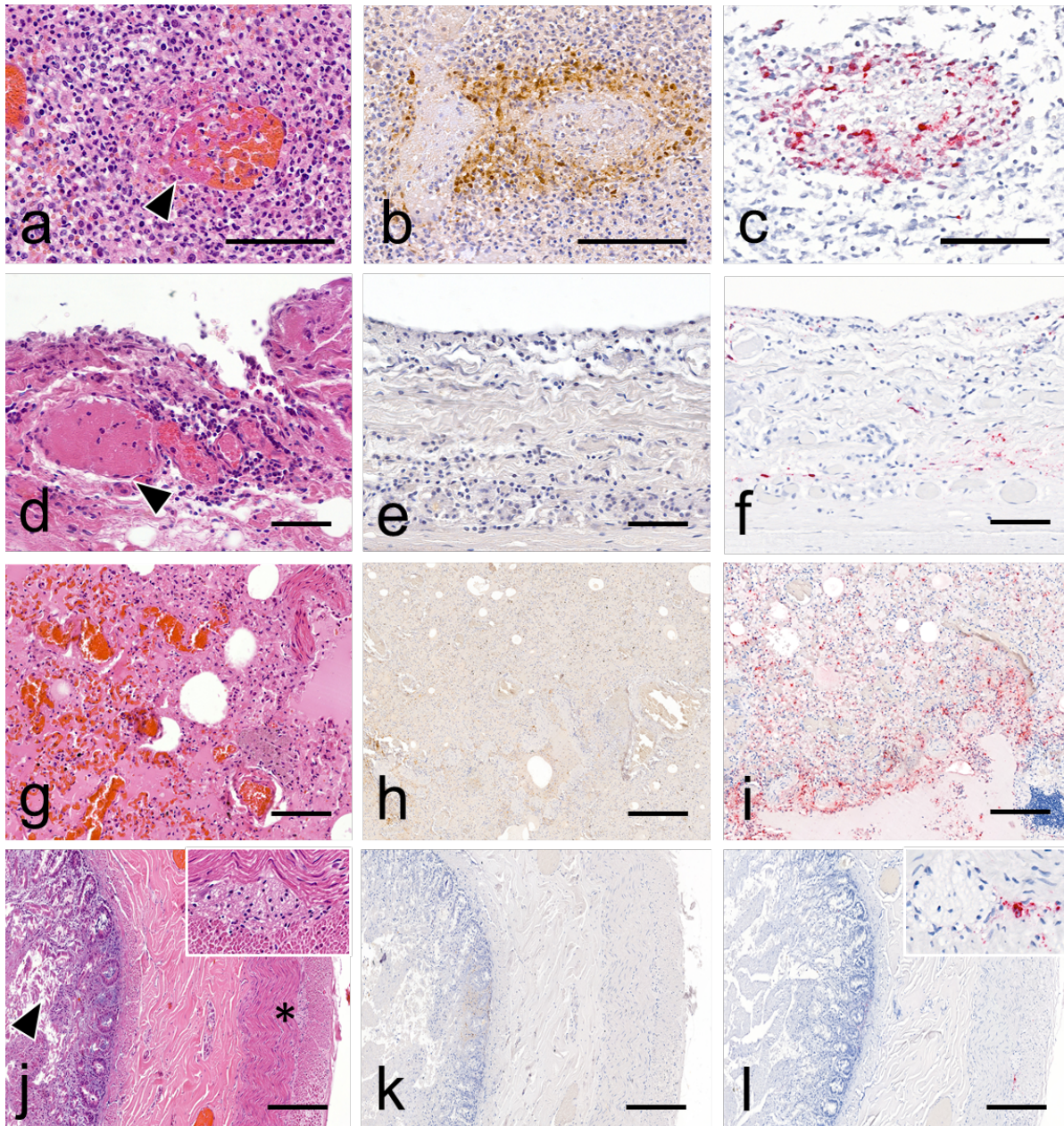


**Figure 1. Histopathology, viral antigen and RNA detection in tissues obtained from infected bear**

a. Visceral lymph node: necrotizing vasculitis (arrowhead) with thrombosis and hemorrhages. Hematoxylin and eosin (H&E) stain. b. Visceral lymph node: viral antigen is observed associated with vasculitis and extending to the surrounding lympho-nodal parenchyma. Anti-nucleoprotein influenza A immunohistochemistry (anti-NP IHC). c. Visceral lymph node: viral RNA is intralesionally detected within areas of vasculitis. M gene RNAscope *in situ* hybridization (RNAscope ISH). d. trachea: thrombosis (arrowhead) and perivascular leukocytic infiltration are observed within the mucosa and submucosa. The overlying epithelium is sloughed (arrowhead) (H&E stain). e. Trachea: no viral antigen detection is observed (anti-NP IHC). f. Trachea: positive viral RNA detection is observed in the interstitium of mucosa and submucosa (RNAscope ISH). g. Lung: diffuse congestion

and edema (H&E stain). h. Lung: IHC shows moderate non-specific background staining with no significant detection of viral antigen at low magnification (anti-NP IHC). i. Lung: viral RNA is widely distributed within the lobular and interlobular interstitium (RNAscope ISH). Intestine: autolytic changes are present in the mucosa, including cell sloughing (arrowhead). The submucosa, tunica muscularis and serosa appear within normal limits. The myenteric plexus (insert and asterisk) is readily identifiable and also normal (H&E stain). j. Intestine: no viral antigen detection is observed (anti-NP IHC). l. Intestine: Viral RNA is focally present within the myenteric plexus (insert) (RNAscope ISH). Scale bars: 50 $\mu$ m (d-f), 100  $\mu$ m (a-c, g-i), 200  $\mu$ m (j-l).

113

114

#### 115 *Phylogenetic and genetic analyses*

116 We performed next generation sequencing on several bear samples (lymph node, lung, and liver) and  
117 one gull sample (brain), using an Element AVITI sequencer (Element Biosciences, San Diego, CA) and a  
118 2x150 bp paired-end protocol. We found H5N1 virus reads in all samples, in sufficient numbers to  
119 reconstitute whole genome consensus sequences, available under accession numbers OR634756 to  
120 OR634763 and OR634764 to OR634771 for the bear and the gull isolates, respectively. Details of the  
121 viral (>100 reads) and bacterial (>1000 reads) species identified by metagenomics can be found in  
122 **Supplementary File 2**.

123

124 Phylogenetic analysis performed on HA gene segment showed that viruses found on both animals  
125 belonged to clade 2.3.4.4b. The HA sequence of the bear-derived virus shared 99.998% genetic identity  
126 with the HA of the strain detected in the gull, making the bird strain the closest related strain (**Figure**  
127 **2**). This finding was further confirmed by the phylogenetic analysis performed on the other viral  
128 segments, which showed that both strains were closely related to strains circulating in Belgium at that  
129 time (**Supplementary Figure 5**). The whole genome analysis revealed both strains belonged to the AB  
130 genotype (H5N1-A/duck/Saratov/29-02/2021-like), the main circulating genotype at that time in  
131 Europe [6].

132

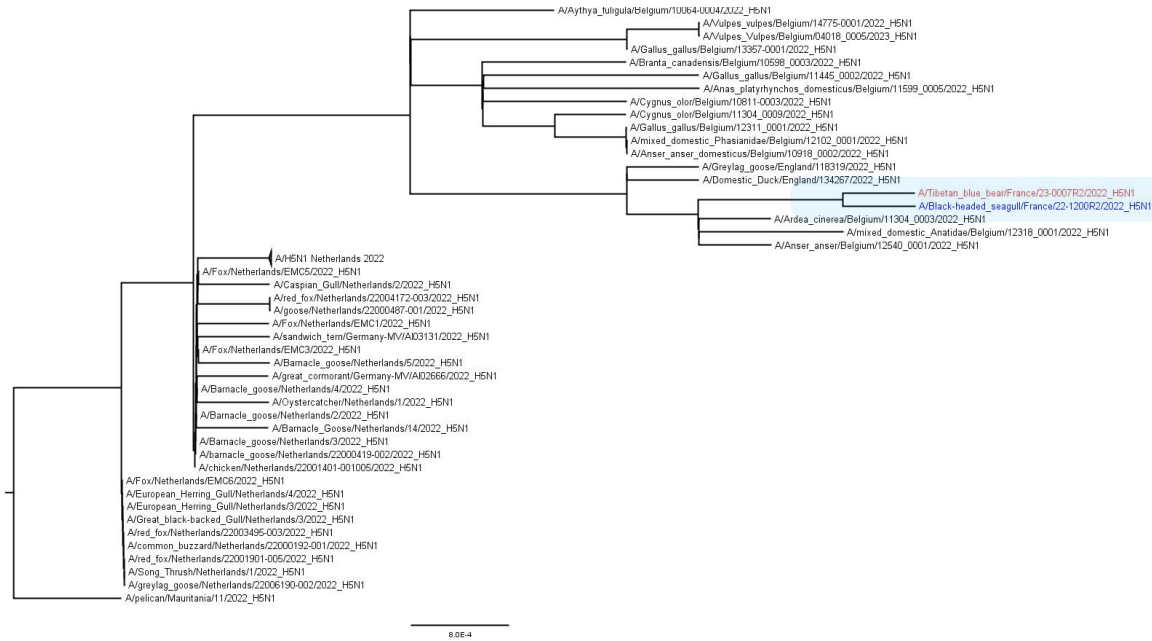


**Figure 2: HA maximum likelihood phylogenetic tree.** Bear and gull-derived sequences are labelled in red and blue respectively. Scale bar: number of nucleotide substitution per site.

133

134

135 Analysis of the consensus sequences revealed the presence of several mammalian adaptation markers,  
 136 listed in **Table 1**, in both bear and gull viruses, markers also found in the genomes of other  
 137 phylogenetically related avian viruses. However, only the bear virus possessed the PB2 E627K marker,  
 138 suggesting that this mutation had emerged over the course of infection.

139

140 We then looked for the presence of minority variants using variant calling analysis. While this analysis  
 141 did not reveal any other mammalian adaptation markers already described in the literature, it did show  
 142 the presence of variants with either an E or a K at position 627 of the PB2 protein, in both bear and  
 143 gull viruses (**Supplementary File 3**). More specifically, in the gull, over 99% of reads coded for an E,  
 144 while in the bear, 37.3% coded for an E and 62.7% coded for a K at position 627, both in the liver and  
 145 lung samples. Although the sequencing depth at this position was around 1400 reads, no sequence  
 146 encoding an E at position 627 was found in the lymph node sample.

147

148

149 **Table 1: Mammalian adaptation markers found on the gull and bear derived viral sequences.** HA  
 150 sequence numbering was performed including the peptide signal.

Protein	Amino-acid position	Gull	Bear	Reference
---------	---------------------	------	------	-----------

PB2	627	E	K	[15]
PB1-F2	66	S	S	[16]
HA	149	A	A	[17]
	170	N	N	[18]
	172	A	A	
M1	30	D	D	[19]
	215	A	A	
NS1	42	S	S	[20]
	92	D	D	[21]
	103	F	F	[22]
	106	M	M	

151

152

### 153 Discussion

154 We revealed the presence of clade 2.3.4.4b H5N1 virus in various tissues of a Tibetan black bear and a  
155 black-headed gull, using histopathology, two different *in-situ* detection techniques and next  
156 generation sequencing. Sequence analysis revealed that the viruses found in the bear and gull were  
157 phylogenetically very close, and that variants with the PB2 E627K mutation had emerged in the bear.  
158 Our findings do not allow us to determine with any certainty how the bear became infected, especially  
159 as the gull was found dead several days after the bear. The most plausible hypothesis is that the virus  
160 circulated undetected for several days in the zoo's wild and captive avifauna, and that the bear was  
161 either in direct contact with an infected bird (dead or alive), or in contact with water or food  
162 contaminated by avian droppings. Interestingly, the PB2 E627K mutation was present in very small  
163 amounts in the gull sample, whereas it was predominant in the bear lung sample. We therefore believe  
164 that it did not arise in the bear through *de novo* mutations, but that the bear's infection was seeded  
165 by an inoculum containing PB2 627E variants and a few PB2 627K variants, which were then selected  
166 because of their selective advantage [15]. Interestingly, the bear lymph node sample contained no PB2  
167 627E variants. This suggests that the PB2 627K variant was selected in the respiratory tract, from which  
168 it then spread systemically.

169



170 When an animal is necropsied outside a research facility, improper preservation of samples is a  
171 frequent issue, especially if the carcasses cannot be refrigerated and if the analysis cannot be  
172 performed quickly. One of the advantages of formalin-fixed paraffin-embedded specimens is that they  
173 can be stored at room temperature for years, if not decades, and are shipped easily [27]. Although this  
174 process degrades the nucleic acids to some extent, methods for extracting DNA and RNA of sufficient  
175 quality are now available [28]. This is how we managed to use FFPE tissues to reconstruct an H5N1  
176 avian influenza virus outbreak in a zoological park through molecular investigations, despite the  
177 absence of fresh tissue samples.

178  
179 Another limitation of our study is that the bear's brain was not examined and sampled. Collecting this  
180 organ would have been technically challenging and since the zoo's veterinary service did not suspect  
181 an infection with an avian influenza virus, at the time of the necropsy, the cranium was not opened.  
182 However, the involvement of the central nervous system has been frequently identified in both birds  
183 and mammals infected with an H5Nx virus of clade 2.3.4.4b, with neurological disorders sometimes  
184 being the only clinical signs observed [28]. For this reason, highlight the presence of the virus and  
185 concurrent histopathological lesions in the brain of our bear would have been of particular interest.

186  
187 In zoological parks many species may reside in close proximity to one another and avoiding contact  
188 with wild birds is difficult, if not impossible, when animals are not kept in cages, but in open spaces.  
189 Zookeepers should receive proper training in biosecurity and made aware of the threats posed by avian  
190 influenza viruses toward mammals, as they were towards SARS-CoV-2 during the COVID-19 pandemic  
191 [29]. This aspect is important, not only for protecting animals, particularly in case of endangered  
192 species, but also for preventing epizootic flare-ups. As the RNA polymerase of influenza viruses is prone  
193 to errors during viral genome replication, better adapted variants may appear when a mammal is  
194 infected by an avian influenza virus [30]. When such a virus spreads from mammal to mammal, the risk  
195 of a more transmissible variant being selected increases considerably, and chains of transmission must  
196 be avoided as much as possible [31]. By raising awareness among veterinarians and zookeepers of the  
197 clinical presentations associated with H5Nx virus infection in mammals, the number of undetected  
198 epizootics should be reduced, with zoological parks thus acting as sentinels.

199  
200 In conclusion, biosecurity and surveillance programs are essential to deal with epizootics caused by  
201 clade 2.3.4.4b H5Nx viruses, and the zoonotic spillovers that are becoming increasingly frequent. In  
202 particular, active and passive surveillance of mammals, including both wild, captive and domestic, will  
203 be invaluable in anticipating the emergence of H5Nx viruses with pandemic potential [33].

204

## 205 **Materials and methods**

### 206 *Histopathology*

207 Tissue samples were placed in 10% neutral buffered formalin. For the bear, available tissues included  
208 trachea, lung, heart, visceral lymph node, spleen, intestine, stomach and kidney. For the gull brain,  
209 trachea, lung, heart, spleen, pancreas (splenic lobe), thyroid gland, liver, intestine and kidney were  
210 collected. After fixation, tissues were routinely processed in paraffin blocks, sectioned at 3µm, stained  
211 with hematoxylin and eosin (H&E) and examined by light microscopy.

### 212 *Immunohistochemistry*

213 To assess viral antigen tissue distribution within the bear and gull tissues, immunohistochemistry (IHC)  
214 was performed on formalin-fixed paraffin-embedded (FFPE) tissue sections, using a monoclonal mouse  
215 anti-nucleoprotein influenza A virus antibody (Biozol BE0159, pronase 0.05% retrieval solution, 10 min  
216 at 37°C: antibody dilution 1/2000, incubation overnight at 4°C). The immunohistochemical staining was  
217 revealed with HRP labeled polymer (EnVisio+ Dual Link System HRP, K4061, Agilent) and the  
218 diaminobenzidine HRP chromogen (DAB+ liquid, K3467, Agilent). Negative controls included sections  
219 incubated either without the primary antibody or with another monoclonal antibody of the same  
220 isotype (IgG2).

221

### 222 *RNAscope ISH*

223 To determine the presence of Avian Influenza A Virus RNA and assess its distribution within the bear  
224 tissue sections, RNAscope *in situ* hybridization (RNAscope ISH) was performed as previously described  
225 [23]. Briefly, we used probes targeting M1 and M2 genes (V-InfluenzaA-H5N8-M2M1 probe), H5  
226 hemagglutinin gene (V-InfluenzaA-H5N8-HA-O1 probe) of clade 2.3.4.4b HPAIV H5 and a RNAscope 2.5  
227 high-definition red assay, according to the manufacturer's instructions, including mild pretreatment  
228 conditions (15 min incubation with protease digestion for antigenic retrieval) and hematoxylin  
229 counterstaining. A probe targeting the dihydrodipicolinate reductase (dapB) gene from the *Bacillus*  
230 *subtilis* strain SMY, served as negative control.

231

### 232 *Next generation sequencing*

233 Three bear samples and one gull sample were selected for the metagenomics analysis on the RNA  
234 fraction: lymph node (bear), lung (bear), liver (bear) and brain (gull). One bear sample (liver) was  
235 selected for the metagenomics analysis on the DNA fraction.

236 The nucleic acids were extracted from the FFPE tissue sections using the Nucleospin total RNA FFPE XS  
237 (Macherey-Nagel). RNA sequencing libraries were prepared using the NEBNext® Ultra™ II Directional  
238 RNA Library Prep Kit (New England Biolabs) and the DNA library was prepared using the NEBNext®

239 Microbiome DNA Enrichment Kit (New England Biolabs). The sequencing run was then performed on  
240 the Element AVITI sequencer (Element Biosciences, San Diego, CA) using a 2x150 bp paired-end  
241 protocol.

242

### 243 *Bioinformatics analysis*

244 The metagenomic data analysis was performed with Kraken2 [24]. We set a threshold at 100 and 1000  
245 reads for the abundance of the viral and bacterial species, respectively. The reads were then mapped  
246 on a H5N1 reference genome (GISAID isolate ID: EPI\_ISL\_17233426) with minimap2 [25] and the  
247 consensus sequences were generated using iVar [26].

248

### 249 *Phylogenetic analysis*

250 Consensus sequences of each viral gene segment detected in black bear were compared with the most  
251 related sequences available in GISAID (<https://www.gisaid.org/>) and aligned by using MAFFT version 7  
252 (<https://mafft.cbrc.jp/alignment/server/index.html>). Maximum-likelihood phylogenetic trees were  
253 generated using RaxML, version 8.2.X (<https://sco.h-its.org/exelixis/software.html>), with a GTR model  
254 associated with gamma distribution (<https://github.com/tamuri/treesub/blob/master/README.md>).  
255 Phylogenetic trees were then visualized by using FigTree version 1.4.2.

256

257

### 258 **Acknowledgment**

259 This study was performed in the framework of the “Chaire de Biosécurité et Santé Aviaires”, hosted by  
260 the National Veterinary College of Toulouse (ENVT) and funded by the Direction Générale de  
261 l’Alimentation, Ministère de l’Agriculture et de la Souveraineté Alimentaire, France.

262 The authors would like to thank HELIXIO SAS (Saint Beauzire—France) for performing the  
263 metagenomics analysis.

264

### 265 **Author contributions**

266 P.B., N.G., G.C., M.C., J.L.G. and G.L.L. conceptualized and designed experiments. P.B., N.G., G.C., M.C.,  
267 M.F.B., M.D., K.L., M.B., P.D. performed experiments. P.B., N.G., M.C., Y.A.M., G.C., M.F.B., K.L., J.L.G.  
268 and G.L.L. analyzed data. J.L.G. and G.L.L. acquired funding. P.B., N.G., M.C. and G.C. drafted the  
269 manuscript. All authors reviewed and edited the final manuscript before submission.

270

### 271 **Competing interests**

272 The authors declare no competing interest.

273

274 **References**

- 275 1. Long JS, Mistry B, Haslam SM, Barclay WS. Host and viral determinants of influenza A virus species  
276 specificity. *Nature Reviews Microbiology*. 2019;17:67–81.
- 277 2. Swayne DE, Suarez DL. Highly pathogenic avian influenza. *Rev Sci Tech*. 2000;19:463–82.
- 278 3. Swayne DE. Understanding the Complex Pathobiology of High Pathogenicity Avian Influenza  
279 Viruses in Birds. *Avian Diseases*. 2007;51:242–9.
- 280 4. Suarez DL. Avian influenza: our current understanding. *Animal Health Research Reviews*.  
281 2010;11:19–33.
- 282 5. Shi W, Gao GF. Emerging H5N8 avian influenza viruses. *Science*. 2021;372:784–6.
- 283 6. EFSA. Avian influenza overview December 2022 – March 2023 | EFSA. 2023.  
284 <https://doi.org/10.2903/j.efsa.2023.7917>.
- 285 7. Bordes L, Vreman S, Heutink R, Roose M, Venema S, Pritz-Verschuren SBE, et al. Highly Pathogenic  
286 Avian Influenza H5N1 Virus Infections in Wild Red Foxes (*Vulpes vulpes*) Show Neurotropism and  
287 Adaptive Virus Mutations. *Microbiology Spectrum*. 2023;11:e02867-22.
- 288 8. Puryear W, Sawatzki K, Hill N, Foss A, Stone JJ, Doughty L, et al. Highly Pathogenic Avian Influenza  
289 A(H5N1) Virus Outbreak in New England Seals, United States. *Emerg Infect Dis*. 2023;29:786–91.
- 290 9. Agüero M, Monne I, Sánchez A, Zecchin B, Fusaro A, Ruano MJ, et al. Highly pathogenic avian  
291 influenza A(H5N1) virus infection in farmed minks, Spain, October 2022. *Euro Surveill*. 2023;28.
- 292 10. Domańska-Blicharz K, Świętoń E, Świątalska A, Monne I, Fusaro A, Tarasiuk K, et al. Outbreak of  
293 highly pathogenic avian influenza A(H5N1) clade 2.3.4.4b virus in cats, Poland, June to July 2023.  
294 *Eurosurveillance*. 2023;28:2300366.
- 295 11. Lindh E, Lounela H, Ikonen N, Kantala T, Savolainen-Kopra C, Kauppinen A, et al. Highly  
296 pathogenic avian influenza A(H5N1) virus infection on multiple fur farms in the South and Central  
297 Ostrobothnia regions of Finland, July 2023. *Eurosurveillance*. 2023;28:2300400.
- 298 12. Jakobek BT, Berhane Y, Nadeau M-S, Embury-Hyatt C, Lung O, Xu W, et al. Influenza A(H5N1)  
299 Virus Infections in 2 Free-Ranging Black Bears (*Ursus americanus*), Quebec, Canada - Volume 29,  
300 Number 10—October 2023 - *Emerging Infectious Diseases journal - CDC*.  
301 <https://doi.org/10.3201/eid2910.230548>.
- 302 13. Leguia M, Garcia-Glaessner A, Muñoz-Saavedra B, Juarez D, Barrera P, Calvo-Mac C, et al. Highly  
303 pathogenic avian influenza A (H5N1) in marine mammals and seabirds in Peru. *Nat Commun*.  
304 2023;14:5489.
- 305 14. Krammer F, Schultz-Cherry S. We need to keep an eye on avian influenza. *Nat Rev Immunol*.  
306 2023;23:267–8.
- 307 15. Hatta M, Gao P, Halfmann P, Kawaoka Y. Molecular Basis for High Virulence of Hong Kong H5N1  
308 Influenza A Viruses. *Science*. 2001;293:1840–2.
- 309 16. Varga ZT, Grant A, Manicassamy B, Palese P. Influenza virus protein PB1-F2 inhibits the induction  
310 of type I interferon by binding to MAVS and decreasing mitochondrial membrane potential. *J Virol*.  
311 2012;86:8359–66.

- 312 17. Yang Z-Y, Wei C-J, Kong W-P, Wu L, Xu L, Smith DF, et al. Immunization by avian H5 influenza  
313 hemagglutinin mutants with altered receptor binding specificity. *Science*. 2007;317:825–8.
- 314 18. Wang W, Lu B, Zhou H, Suguitan AL, Cheng X, Subbarao K, et al. Glycosylation at 158N of the  
315 hemagglutinin protein and receptor binding specificity synergistically affect the antigenicity and  
316 immunogenicity of a live attenuated H5N1 A/Vietnam/1203/2004 vaccine virus in ferrets. *J Virol*.  
317 2010;84:6570–7.
- 318 19. Fan S, Deng G, Song J, Tian G, Suo Y, Jiang Y, et al. Two amino acid residues in the matrix protein  
319 M1 contribute to the virulence difference of H5N1 avian influenza viruses in mice. *Virology*.  
320 2009;384:28–32.
- 321 20. Jiao P, Tian G, Li Y, Deng G, Jiang Y, Liu C, et al. A single-amino-acid substitution in the NS1 protein  
322 changes the pathogenicity of H5N1 avian influenza viruses in mice. *J Virol*. 2008;82:1146–54.
- 323 21. Seo SH, Hoffmann E, Webster RG. Lethal H5N1 influenza viruses escape host anti-viral cytokine  
324 responses. *Nat Med*. 2002;8:950–4.
- 325 22. Kuo R-L, Krug RM. Influenza A virus polymerase is an integral component of the CPSF30-NS1A  
326 protein complex in infected cells. *J Virol*. 2009;83:1611–6.
- 327 23. Gaide N, Crispo M, Jbenyeni A, Bleuart C, Delverdier M, Vergne T, et al. Validation of an  
328 RNAscope assay for the detection of avian influenza A virus. *J VET Diagn Invest*.  
329 2023;:10406387231182385.
- 330 24. Wood DE, Lu J, Langmead B. Improved metagenomic analysis with Kraken 2. *Genome Biology*.  
331 2019;20:257.
- 332 25. Li H. Minimap2: pairwise alignment for nucleotide sequences. *Bioinformatics*. 2018;34:3094–100.
- 333 26. Grubaugh ND, Gangavarapu K, Quick J, Matteson NL, De Jesus JG, Main BJ, et al. An amplicon-  
334 based sequencing framework for accurately measuring intrahost virus diversity using PrimalSeq and  
335 iVar. *Genome Biology*. 2019;20:8.
- 336 27. Donczo B, Guttman A. Biomedical analysis of formalin-fixed, paraffin-embedded tissue samples:  
337 The Holy Grail for molecular diagnostics. *Journal of Pharmaceutical and Biomedical Analysis*.  
338 2018;155:125–34.
- 339 28. Farragher SM, Tanney A, Kennedy RD, Paul Harkin D. RNA expression analysis from formalin fixed  
340 paraffin embedded tissues. *Histochem Cell Biol*. 2008;130:435–45.
- 341 29. Foret-Lucas C, Figueroa T, Coggon A, Houffschmitt A, Dupré G, Fusade-Boyer M, et al. In Vitro and  
342 In Vivo Characterization of H5N8 High-Pathogenicity Avian Influenza Virus Neurotropism in Ducks and  
343 Chickens. *Microbiol Spectr*. 11:e04229-22.
- 344 30. Dusseldorp F, Bruins-van-Sonsbeek LGR, Buskermolen M, Niphuis H, Dirven M, Whelan J, et al.  
345 SARS-CoV-2 in lions, gorillas and zookeepers in the Rotterdam Zoo, the Netherlands, a One Health  
346 investigation, November 2021. *Eurosurveillance*. 2023;28:2200741.
- 347 31. Bessièrè P, Volmer R. From one to many: The within-host rise of viral variants. *PLOS Pathogens*.  
348 2021;17:e1009811.

349 32. Russell CA, Fonville JM, Brown AEX, Burke DF, Smith DL, James SL, et al. The Potential for  
350 Respiratory Droplet–Transmissible A/H5N1 Influenza Virus to Evolve in a Mammalian Host. *Science*.  
351 2012;336:1541–7.

352 33. Hay AJ, McCauley JW. The WHO global influenza surveillance and response system (GISRS)—A  
353 future perspective. *Influenza and Other Respiratory Viruses*. 2018;12:551–7.

354